Biomass Conversion and Biorefinery (2023) 13:2687–2702
https://doi.org/10.1007/s13399-021-01323-1

ORIGINAL ARTICLE

Biodegradation efficacy of coke oven wastewater inherent co-cultured novel sp. *Alcaligenes faecalis JF339228* and *Klebsiella oxytoca KF303807* on phenol and cyanide—kinetic and toxicity analysis

Uttarini Pathak[1] · Patali Mogalapalli[1] · Dalia Dasgupta Mandal[2] · Tamal Mandal[1]

Received: 23 October 2020 / Revised: 8 January 2021 / Accepted: 22 January 2021 / Published online: 10 February 2021

Abstract

Coke oven sector emanates phenol and cyanide as the eminent virulent compounds due to abrupt industrialization which is detrimental in aqueous state, and its severity is increased on simultaneous coexistence even at low concentrations that eventually causes extensive damage to the peripheral ecosystem. The efficacy of isolated mixed bacterial culture comprising of *Alcaligenes faecalis* JF339228 and *Klebsiella oxytoca* KF303807 in wastewater treatment was investigated following a batch study. The impact of initial concentration of phenol (100–1500 mg L^{-1}) and cyanide (10–150 mg L^{-1}) on the growth and treatment by the mixed microbial cultures were evaluated over a time period of 72 h. The biodegradation mechanism was explained by Monod, Haldane, Aiba and Edward kinetic models. The maximum specific growth rate was reported to be 0.096 h^{-1} and 0.126 h^{-1} for phenol and cyanide respectively. The substrate inhibitory effect became eminent after a concentration of 450 mg L^{-1} for phenol and 45 mg L^{-1} for cyanide. Based on the lower sum of squared error (SSE) values, Haldane model for phenol and Edward model for cyanide was found to be favourable for substrate inhibition kinetics. The fate of the secondary intermediates produced after microbial degradation was assessed by phytotoxicity studies using *Vigna radiata*. The interactive binding of the pernicious pollutants and resultant biodegraded compounds with the DNA (herring sperm DNA) was examined following spectrofluorometric and spectrophotometric anatomization. Toxicity studies revealed that biological treatment was viable for eco benign disposal and results also depicted that both the strains have potential in remediation of phenol and cyanide from coke oven wastewater.

Keywords Phenol · Cyanide · *Alcaligenes faecalis* JF339228 · *Klebsiella oxytoca* KF303807 · Kinetics · Toxicology

1 Introduction

The existence of phenol and cyanide in different industrial discharges becomes an eminent problem when released to the environment from major sectors like oil and petrochemical, solvent and paint, pharmaceutical, mining, pesticides and explosives units [1–7]. However, the contribution of coke oven and steel manufacturing industries has been found to be most significant with a range of 300–500 mg L^{-1} of phenol and 10–50 mg L^{-1} of cyanide respectively [8–10]. The inflated levels of these toxicants have a consequential impact on the flora and fauna when the industrial discharge exceeds more than the natural degradation rate causing these substances to accumulate in the environment. The virulent effects of phenol and cyanide as observed on humans include severe damage to cardiac, gastrointestinal and central nervous systems; major organs like the liver, kidney, skin and eye; and especially respiratory system as the cytochrome oxidase is targeted by potential toxicity [11, 12]. The exorbitant limits of phenol and cyanide in the industrial effluent have caused several environmental organizations to impose a prohibitive limit (MCL or maximum contaminant level) of 0.5 mg L^{-1} and 0.2 mg L^{-1} respectively [13, 14].

✉ Tamal Mandal
tamal.mandal@che.nitdgp.ac.in; https://orcid.org/0000-0002-0493-747X

[1] Department of Chemical Engineering, NIT Durgapur, Durgapur, India

[2] Department of Biotechnology, NIT Durgapur, Durgapur, India

The elimination of these complex toxicants has become a stimulating challenge for researchers to drift from prevalent abatement strategies like adsorption [15, 16], physico-chemical separation [17–20] and chemical oxidation [21] towards bioremediation [22]. Biological treatment is associated with low-cost conversion of toxic compounds into non-toxic metabolites without sludge generation and can function in a broad range of operating parameters especially bacteria [23]. They involve no chemical handling and are site specific requiring proper evaluation of process parameters like nutrient balance, substrate concentration and availability, viscosity, exposure to additional toxic contaminants and especially temperature and pH of the environment [24]. Bioremediation associated with selection of suitable strain simplifies the process satisfying the ultimate requirement of separation and environmental control. The implementation of these processes is occurring on a large engineered scale owing to the favourable volumetric reaction rates and overall productivity of suspended cultures [25]. Several literature reports about the wide application of *Pseudomonas* sp., for degrading phenol and cyanide in batch and continuous mono substrate systems [26–30]. The most recent study by Singh et al. [31] reports about the degradation potential of *Pseudomonas putida* and *Pseudomonas stutzeri* isolated from coke oven effluent–contaminated soil for 720 mg L^{-1} phenol and 37 mg L^{-1} cyanide in binary system with 80% degradation simultaneously. Other microbial species implemented in bioremediation of phenol-cyanide system are specified in Table 1. The rate of biodegradation is comparatively deflated in binary substrate system owing to competitive substrate inhibition and toxicity with reduced biomass growth and yield [32]. Moreover, the coexistence of phenol and cyanide in combination with various other pollutants typically complicates its removal and urges for the need of its eradication in a binary system.

The current research deals with a binary substrate system containing simulated aqueous phenol and cyanide to be degraded by a mixed isolated bacterial consortium *Alcaligenes faecalis* JF339228 and *Klebsiella oxytoca* KF303807 which has not been reported earlier. The concept of implementing these potential degraders for specific bio-remediative action of phenol and cyanide simultaneously in a batch process emerged to be effective. Though several pure and mixed cultures have been applied for degradation study, strategic selection of specific degraders for target phenol and cyanide systems was the novel approach and has not been attempted earlier. The detailed substrate growth kinetic study of the microbial culture was performed following Monod, Haldane, Aiba and Edward kinetic models. The intent of this study was to apprehend the impact of the toxicants on microbial metabolism in a binary substrate system and the interference caused by the substrate interactions. The fate of the pollutants and biodegraded compounds for eco benign disposal was further assured by toxicological study on plant and aquatic DNA system. The bioattenuation of phenol and cyanide using the assorted isolated bacterial strains having its origin in coke oven wastewater emerged with a new dimension.

2 Materials and methods

2.1 Chemicals and reagents

The chemicals and reagents used for this study were of high analytical grade with 99% purity procured from Merck, India Ltd. The stock solution of phenol was prepared by dissolving phenol crystals (Merck, India Ltd.) in 1 l of double-distilled water. Thermo Fischer Scientific 1000 ppm standard cyanide solution was procured which was used by further serial dilution. The overall stock solution was preserved in a laboratory grade brown glass bottles covered by foil to avoid any material loss by photo-oxidation. Standard stock solution of phenol and cyanide having pH in the range of 7.2–7.56 was prepared regularly without any further adjustment by HCl or NaOH solutions. Simulated wastewater containing phenol and cyanide concentration ranging from 50 to 1500 mg $L^{-1}$and 5 to 150 mg L^{-1} was synthesized where the concentration was retained in 10:1 ratio as present in the industrial wastewater. The growth media were maintained at pH 7.0±0.2 for the mineral salt medium (MSM) consisting of ammonium sulphate ($(NH4)_2SO_4$), dipotassium hydrogen phosphate (K_2HPO_4), potassium dihydrogen phosphate (KH_2PO_4), magnesium chloride ($MgCl_2{\cdot}7H_2O$) and calcium chloride ($CaCl_2{\cdot}2H_2O$) as reported by [38]. Phytotoxicity studies were performed using *Vigna radiata* purchased from local markets of Durgapur. The Herring sperm DNA (hs-DNA) was supplied by Sigma-Aldrich Co. (USA) and Ethidium Bromide (EtBr) dye from Himedia Ltd. India.

2.2 Microorganism isolation and cultivation

Alcaligenes faecalis JF339228 and *Klebsiella oxytoca* KF303807 were isolated from coke oven and steel plant wastewater of Durgapur and IISCO, Burnpur, respectively. The bacterial strains were isolated in the laboratory at NIT Durgapur (23.5477° N, 87.2931° E), India, following serial dilution method. The individual pure microbial cultures were incubated at a temperature of 35 °C, 140 rpm over a period of 72 h to allow maximum growth in a sterile medium comprising of beef extract (1.5 g L^{-1}), yeast extract (1.5 g L^{-1}), sodium chloride (5 g L^{-1}) and peptic digest of animal tissue (5 g L^{-1}). Only the fully developed cultures from the late exponential phase were considered for transfer to the mineral salt medium (MSM) for acclimatization and biodegradation studies. Before transferring to the mineral salt medium, the cellular biomass was subjected to washing with phosphate-buffered saline solution (pH 7.4). The mixed strains were grown in

Table 1 Different bacterial species involved in bioremediation of phenol-cyanide system

Microbial species	Target pollutant	Reference
Pseudomonas putida MTCC 1194	Phenol and cyanide degradation	[32];
Pseudomonas sp.	Phenol	[29]; [27]; [28] [33] [34] [35]
Serratia odorifera MTCC 5700	Phenol and cyanide degradation	[36]
Alcaligenes	Phenol	[37] [38] [39]
Pseudomonas stutzeri	Phenol	[40] [31]
Ralstonia eutropha	Phenol	[41]
R. erythropolis	Phenol	[42]
Comamonas	Phenol	[30]
Klebsiella oxytoca	Cyanide	[43] [11]
Bacillus sp.	Cyanide	[44] [45]
Pseudomonas fluorescens	Cyanide	[46]

pre-sterilized (in an autoclave at 121 °C temperature; 15 psi pressure for 15 min) mineral salt medium (MSM) for batch degradation of phenol and cyanide under aerobic conditions. The same media composition was accompanied with phenol (50–1500 mg L^{-1}) and cyanide (5–150 mg L^{-1}) for acclimatization of the bacterial cultures at varying concentration. All operations concerning transfer of inoculum were carried out in a laminar chamber with air flow unit. Initially, glucose was the only source of carbon for the mixed strains. The glucose content was replaced with phenol as the carbon source to allow the co-cultured strains to adapt the final environment. Similarly, the presence of ammonium sulphate $(NH4)_2SO_4$ in the nutrient medium deflates the extent of utilization of cyanide as nitrogen source by the bacteria [11]. Thus, it was replaced by cyanide only for essential nitrogen source. The maintenance of the proper nutritional balance under optimized conditions is vital during bio-treatment and the failure of which can lead to reduced metabolic activity.

2.3 Biodegradation studies and analysis

All biodegradation experiments were performed with the mixed bacterial consortium cultured in minimal nutrient salt media and subjected to various concentrations of phenol and cyanide where the volume of the added microbial culture was maintained uniform throughout. The growth and degradation studies were executed for a period of 72 h in a batch shaking medium and the treated samples were collected at regular time intervals. Blank samples containing only aqueous phenol were rotated along with other samples to ensure any loss of volatile phenol in shaker medium. The biomass growth was evaluated by measuring the optical density or absorbance at 600 nm of the turbid sample in a UV-vis spectrophotometer (Agilent technology, Cary 60). For calculation of the dry biomass weight, the cell pellet was separated from the resultant solution following centrifugation at 10000 rpm for 15 min. After washing with distilled water and drying in an oven, the dry cell weight (mg L^{-1}) was obtained to calibrate it against the obtained OD_{600} of biomass. The values of optical density at 600 nm were converted to dried cellular mass from the calibration curve of OD vs dry biomass. The final concentration of phenol was analysed following the standard 4 amino antipyrene method using UV-vis spectrophotometer (Agilent technology, Cary 60) at 460 nm [47]. Cyanide was assessed using Orion Ion digitalized metre with Electrode by Thermo Fischer Scientific [48].

$$\text{Percentage Biodegradation } (\%) = \frac{C_i - C_O}{C_i} \times 100 \quad (1)$$

C_i and C_o denotes the initial and instant concentration of phenol and cyanide.

2.4 Kinetic models

Batch growth kinetic studies were performed to illustrate the growth pattern of the microbial culture in a medium

containing phenol and cyanide by involving models explaining specific growth and substrate degradation rate. The study of growth kinetics plays an essential role in determining the capabilities of microorganism in terms of biodegradation and its operation in pilot scale treatment units. There is a difference in opinion regarding the inhibitory effect of phenol in literatures due to which two approaches arrive—one dealing with non-inhibitory Monod model and the other comprising of growth-inhibitory models like Haldane, Edward and Aiba respectively [49]. Out of the later models, Haldane is extensively used for substrate inhibition study owing to its mathematical simplicity suitable for modelling continuous biological systems. For evaluation of the specific growth rate or μ (h^{-1}) at each initial concentration of phenol and cyanide, ln (S/S_0) was plotted linearly against cell biomass (X) where S_o denotes initial substrate concentration and S is the concentration at any time t for specific S_o. Monod model is extensively used for calculation of growth kinetic parameters and utilization of substrate by microorganisms. However, there is a non-uniqueness over the reliability of kinetic parameters. This function involves a non-inhibitory approach where the growth rate increases with the initial concentration of the substrate asymptotically to a maximum value. The effect of initial pollutant concentration on the specific growth rate was studied by calculating the slope of ln (biomass) vs time which was calculated for each phenol and cyanide concentration during the exponential phase. In Monod model, the specific growth rate or μ (h^{-1}) is expressed in terms of substrate concentration as [50]

$$\mu = \frac{\mu_{\max} S}{K_s + S} \tag{2}$$

$$\mu = \frac{1}{X}\frac{dX}{dt} \tag{3}$$

The maximum growth rate is denoted by μ_{max} for which the gradient of specific growth rate with concentration $\left(\frac{d\mu}{ds} = 0\right)$ is zero.

Owing to the limitation of Monod model applicable for lower substrate concentrations, Haldane model was considered in account of substrate inhibition expressed as [51]

$$\mu = \frac{\mu_{\max} S}{K_s + S + \left(\frac{S^2}{K_i}\right)} \tag{4}$$

K_s and K_i are half saturation and substrate inhibition constant in milligrams per liter. The substrate inhibition constant predicts the limiting threshold value of the concentration up to which the microorganism can resist. This is typically significant for its practical applications above which the concentration limit should not be exceeded. Haldane model defines a curve where the growth rate increases with substrate concentrations up to a certain maximum value after which it declines for further inflation.

The true maximum growth rate S_m at $\left(\frac{d\mu}{ds} = 0\right)$ is [52]

$$S_m = \sqrt{K_S K_i} \tag{5}$$

S_m is the value of concentration corresponding to the maximum growth rate. It suggests the range below which the growth is limited by the substrate and above which the growth is influenced by the substrate inhibition. The value of K_s is directly proportional to the μ_{max} indicating a possible correlation between them.

An improvised form of Haldane model was suggested by Edward model [53, 54]

$$\mu = \mu_{\max} s\left[\exp\left(\frac{-S}{K_i}\right) - \exp\left(\frac{-S}{K_s}\right)\right] \tag{6}$$

Another model suggested by Aiba et al. [55] is illustrated as

$$\mu = \frac{\mu_{\max} S}{K_s + S}\exp\left(\frac{-S}{K_i}\right) \tag{7}$$

The specific substrate degradation rate was evaluated by the following relation using instantaneous biomass (x) and substrate (S) concentrations as [36]:

$$q = \frac{-\ln(x_2 - x_1)}{(S_2 - S_1)} \tag{8}$$

The experiments were performed in triplicate setup so as to maintain accuracy in results with minimum standard error. The fitting and suitability of the models were measured in terms of sum of squared errors (SSEs).

2.5 Instrumental anatomization using scanning electron microscopy

The microscopic morphology of the mixed bacterium was observed using ZEISS EVO-MA 10 scanning electron microscope, Germany. Scanning electron microscopes play a significant role in obtaining images for biofilms developed on nontransparent surfaces with detailed study of complex topology by sectioning optically. Inoculated cultures of *Alcaligenes faecalis* JF339228 and *Klebsiella oxytoca* KF303807 in nutrient broth and acclimatized in phenol and cyanide MSM media post degradation were collected, dried and deposited on oil-free glass sheets to obtain images under vacuum pressure exposed to an electron beam of 15 kV. Dehydration of the specimen is essential as the coatings of the samples are performed in a vacuum chamber so as to produce the surface electrically conducting for the process. The samples were initially coated in an auto fine coater with palladium having thickness 8 nm at the rate of 30 mA for 30 s to enhance the conductivity of the samples. Later it was dried under infrared lamps. Photo micrographs of the untreated and treated samples were captured

under bright-field emission microscope (Dewinter Premium) at × 20 and × 100 magnifications following a gram staining procedure.

2.6 Toxicity assessment and fluorescence spectrophotometer study

The fluorescence spectral analysis was conducted using a working concentration of 60 μM Herring sperm DNA (hs-DNA), a commonly used DNA model from the species of fish *Clupea harengus*, in 100 mM Tris-buffered solution. Agilent Technologies fluorescence spectrophotometer model Cary Eclipse G9800A was used to assess the interaction of the pollutants with hs-DNA in presence of Ethidium Bromide dye (EtBr 2 μM) as fluorophore and determine the fate of the secondary intermediates produced after bioremediation process. The spectral analysis was performed at room temperature where the sample containing the hs-DNA, EtBr dye and the treated/untreated wastewater was prepared following incubation at 37 °C for 10 min. The excitation and emission spectrum was obtained to anatomize the binding activity and attachment of the toxic molecules to the DNA base pairs keeping the total volume and DNA concentration constant. The excitation wavelength in the case of fluorescence spectrophotometer was fixed at 471 nm, and the fluorescence intensity for emission wavelength starting from 480 to 800 nm was recorded for the untreated and microbially treated samples. In the case of UV-visible spectrophotometer, the maximum wavelength for the determination of nucleic acid quantification or DNA purity check is 260 nm in the case of hs-DNA which was used for the detailed interactive study. On keeping the total working volume fixed, the concentration of the wastewater was increased and performed for three different sets of phenol and cyanide concentrations. This helped in maintaining the uniformity of the DNA concentration and acquiring distinguishable characterized bands.

Plant model systems are mostly considered for toxicological study due to their complicated eukaryotic structure. Phytotoxicity study of untreated and microbial remediated samples was performed by germination bioassay using mung bean (*Vigna radiata*) [56]. Initially, the beans were cleaned to get rid of the impurities. 0.1% $HgCl_2$ and 70% ethanol were used for surface sterilization of the 10 number of mung beans accompanied with repeated distilled water washing. The beans were further subjected to soaking in distilled water for 6 h. The surface-soaked beans were uniformly distributed on pre-sterilized Petri plates where equal volumes of untreated and bio-treated samples were applied. Distilled water was added to the control plate. Thirty percent H_2O_2 was considered a positive control. These plates were maintained in a plant growth room at temperature 22 ± 3 °C for 5 days with balanced moisture and light. Equal volume of samples was added to the beans every day for 5 days and both light and dark phases were programmed inside the plant chamber.

Root toxicity was calculated as follows:

$$\%\text{Root Toxicity} = \frac{(\text{Root length of control}) - (\text{Root length of treatment})}{(\text{Root length of control})} \times 100 \quad (9)$$

The length of shoot was measured at final day and shoot toxicity was calculated as follows:

$$\%\text{Shoot Toxicity} = \frac{\text{Shoot length of control} - \text{Shoot length of treatment}}{\text{Shoot length of control}} \times 100 \quad (10)$$

3 Results and discussions

3.1 Morphological study of microbial cell using light and scanning electron microscopy

The scanning electron microscopic analysis of the microbial mass depicted from Fig. 1 a indicated that the surface of the original mixed bacterial culture was porous, rough and heterogeneous with wide network of lumps suggesting preferable surface area for effective binding of toxicants [57]. Amorphous clumps of single celled organisms clustered together were reflected in the scanned electronic images. This type of non-filamentous organisms usually exists in groups with similar structural morphology. They represent microcolonial structures or a part of broader microbial colony as observed in this study.

Both *Alcaligenes faecalis* JF339228 and *Klebsiella oxytoca* KF303807 were reported to be gram-negative bacteria as observed from the microscopic images in Fig. 2a and b following a gram staining procedure and mentioned in the literature [38, 43]. These gram-negative bacteria have reduced peptidoglycan content in their outer membrane which relaxes sensitivity and makes them flexible towards virulent compounds [58, 59]. Thus, in comparison to gram-positive cells, they exhibit less morphological changes when exposed to detrimental environment. Light microscopic examination of the bacterial cells suggested rod-shaped structure with absence of flagella and disrupted chains. From Fig. 1b, the rough surface of the cells was transformed into smooth exterior after bioaccumulation of phenol and cyanide [57, 60]. No other significant changes were discerned from Fig. 2a and b which designates the resilience and potential of the applied bacterial strain.

3.2 Influence of initial concentration

The concentration of phenol and cyanide was varied between 50 and 1500 mg L^{-1} and 5–150 mg L^{-1} respectively to

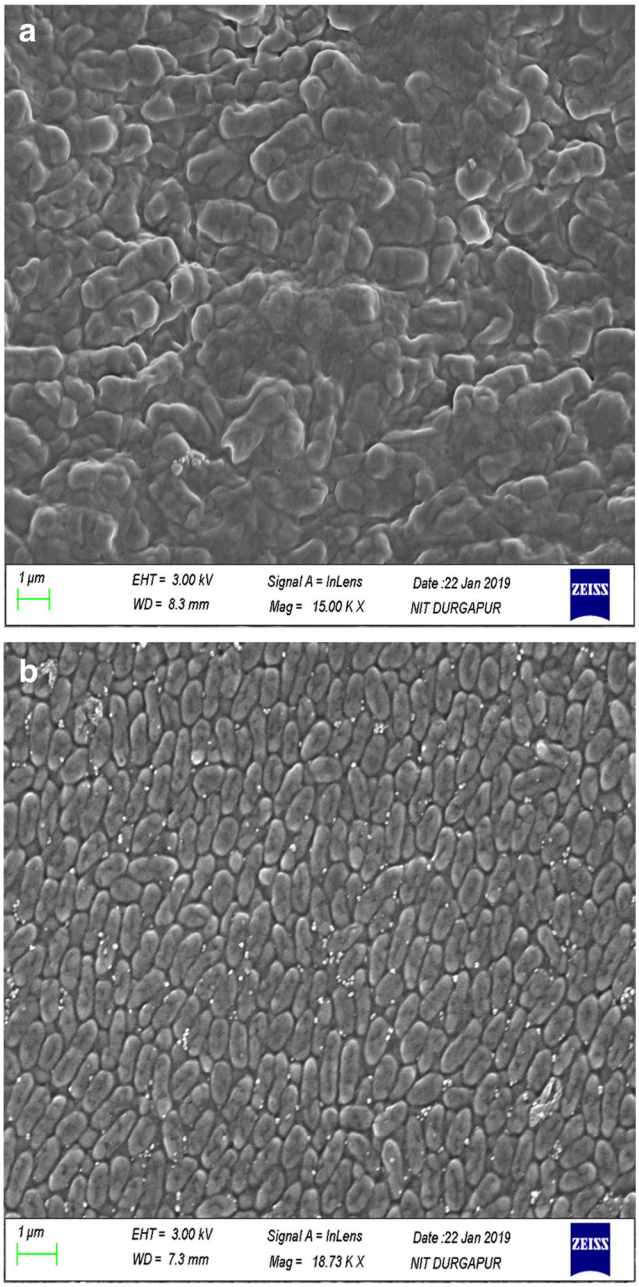

Fig. 1 Scanned electronic images of mixed bacterium **a** before and **b** after biodegradation

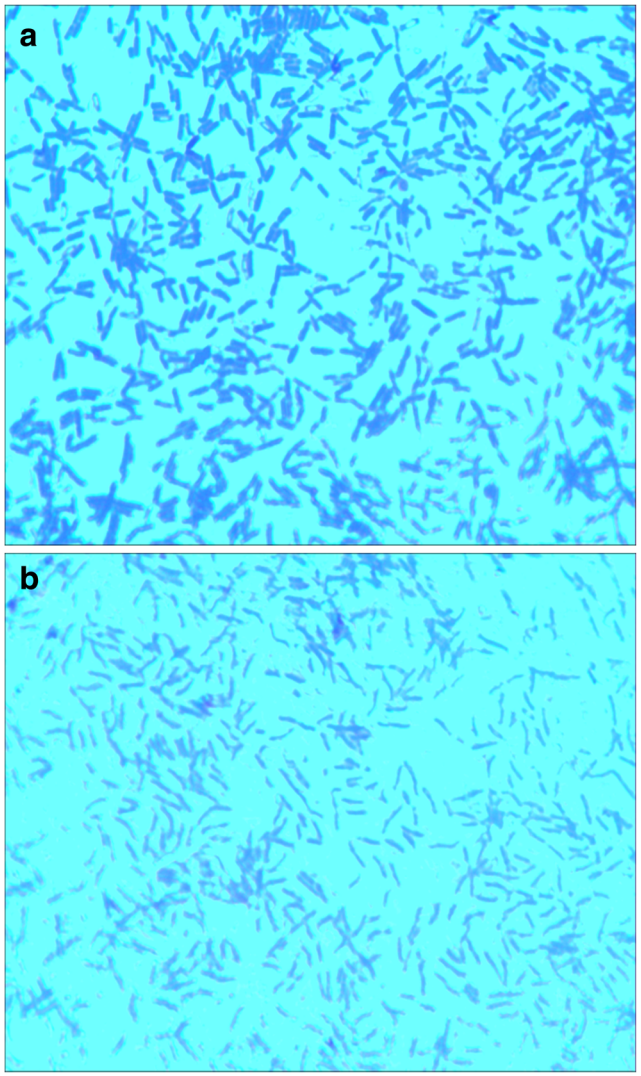

Fig. 2 Photomicrographs of mixed bacterium under bright-field microscope **a** before and **b** after biodegradation

determine the degradability potential for a period of 72 h. Initially, a degradation time of 90 h was provided but no significant changes in the toxicants removal was observed after 72 h. At lower concentrations less than 200 mg L^{-1} phenol and 20 mg L^{-1} cyanide, the degradation efficiency was 100% within 72 h as the microbial growth is high due to lower inhibitory substrate effect which permits the microbes to utilize phenol as carbon-energy medium and cyanide as nitrogen source. A diauxic nature of the microbial community is observed; i.e. for existence of dual carbon resources like glucose and phenol, the microorganism would opt for glucose initially followed by phenol and cyanide media [32]. On the other hand in absence of phenol and glucose, microbes find it difficult to use any other carbon resource and no growth was observed due to the toxicity of cyanide compounds [11].

Figure 3a and b represent the variation of specific growth rate of the mixed consortium at different concentrations of phenol and cyanide. It is evident from Fig. 3a and b that both the growth and degradation rates were agreeable with each other with an substantial increase (Monod growth kinetics in Eq. 2) initially followed by a decline depicting substrate inhibiting features in the growth system [23, 61]. This trend obtained in this figure also indicated that Haldane model can be applied. The substrate is consumed rapidly during the exponential phase which declines at the end with a lower rate of substrate removal due to lower availability of oxygen and reduction in pH affecting the substrate growth-inhibition kinetics. At extreme low substrate concentration, growth will be affected due to unavailability of food and the specific growth

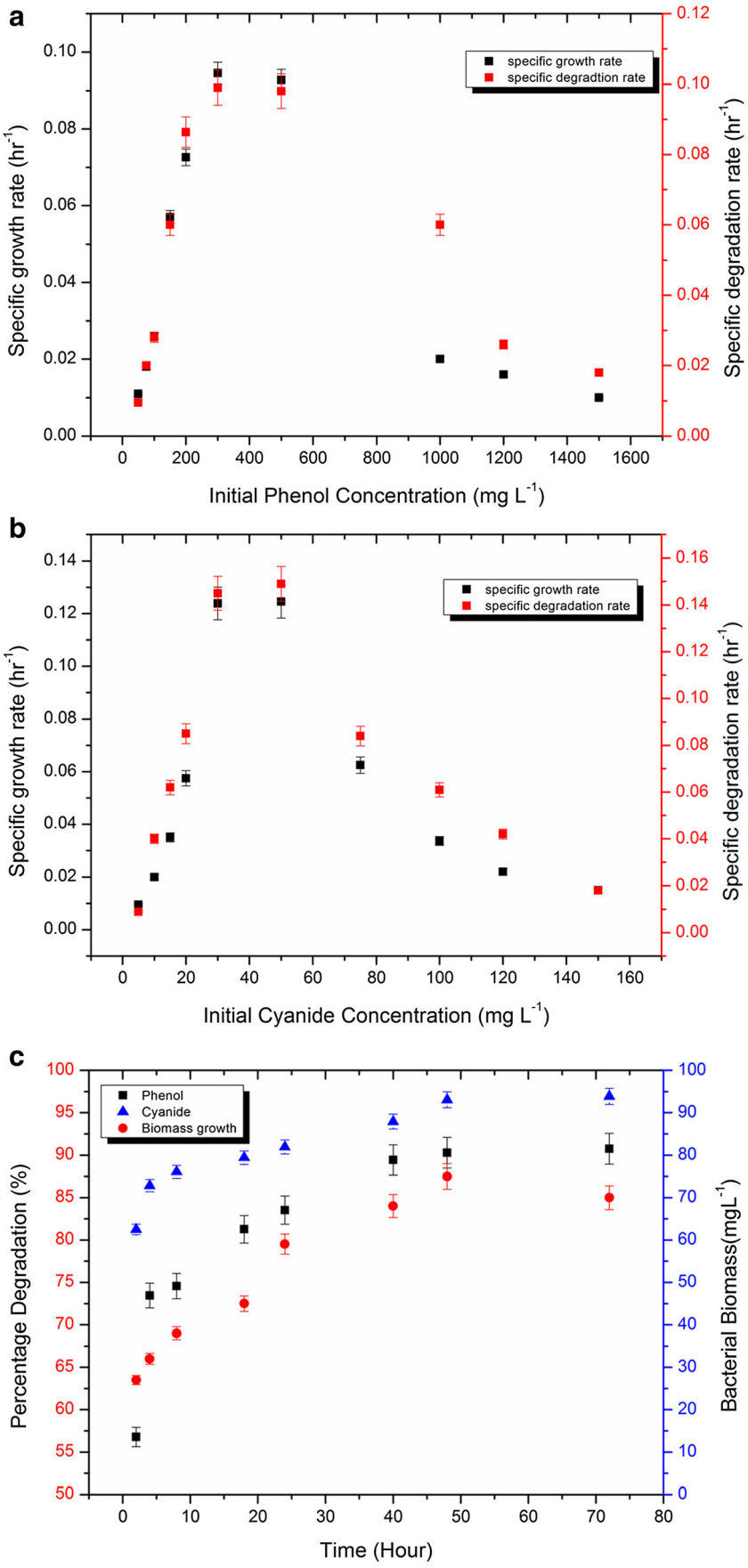

Fig. 3 **a** Influence of initial phenol concentration on specific growth rate and specific substrate degradation rate. **b** Influence of initial cyanide concentration on specific growth rate and Specific substrate degradation. **c** Influence of contact time on percentage degradation of phenol and cyanide using mixed bacterial culture

rate is reduced. Similarly, when the inhibitor (substrate at very high concentrations) comes in contact with a microbial cell, its metabolic activity reduces due to sudden disruption of the permeable barrier. This causes disturbances in the internal composition as well as the transport mechanism of the cell depriving the bacteria of adequate nutrient supply [22].

In this study, the specific growth rate and specific degradation rate initially increased up to 450 mg L^{-1} phenol and 45 mg L^{-1} cyanide respectively. In the case of phenol as the carbon source when the concentration is increased from 50 to 100 mg L^{-1}, the sp. growth rate (μ) enhances by 2.3 times. This factor inflates by 3.6 times until 450 mg L^{-1} phenol (7 carbon folds) due to rapid substrate utilization after which substrate inhibition resumes, and there is a decline by 4.6 times. Similarly, when cyanide is utilized as the nitrogen source and it is changed by the same number of folds, the factor enhances by 0.4 times until 45 mg L^{-1} cyanide after which it declines by a factor of 2.7. The maximum specific growth rate was observed to be $\mu_{max,phenol}$ = 0.096 h^{-1} and $\mu_{max,cyanide}$=0.126 h^{-1} respectively. Kumar et al. [38] has shown results with 100% degradation of 2100 mg L^{-1} of phenol in an incubation period of 90.8 h involving *A. faecalis* JF339228 in a mono substrate system. Christen et al. [52] reported of using a thermoacidophilic strain of *Sulfolobus solfataricus* following aerobic biodegradation of 51–745 mg/l phenol in a batch system with a maximum specific growth rate of 0.047 h^{-1} suggesting the inhibitory nature of phenol in between 93 and 175 mg L^{-1}. [29] performed biological degradation of 1000 mg/l phenol and 500 mg/l catechol by *Pseudomonas putida MTCC 1194* with μ_{max}=0.305 h^{-1}, K_s= 36.2 mg L^{-1} and K_i= 129.79 mg L^{-1} for phenol.

3.2.1 Role of enzymes involved in microbial degradation

Oxygenases are the most significant enzymes in aerobic biodegradation of aromatic hydrocarbons. Phenol is a vital carbon source metabolized by ortho and meta cleavage involving hydroxylase as the prime degrading enzyme accompanied by catechol 1,2 dioxygenase and catechol 2,3 dioxygenase enzymes [62, 63]. On the other hand, nitrogenase is the cyanide-degrading enzyme secreted by *K. oxytoca* KF303807 with simultaneous bicarbonate and ammonia production as an assimilatory substrate [11, 43]. The enzymatic activity is intercellular and is enhanced during the growth phase when the number of microbes increases as a result of which the food intake is high by the microorganisms followed by exponential decay. The similar nature is observed for the specific degradation rate at different concentrations from Fig. 3a and b and Eq. 8. At higher initial concentrations, due to extreme substrate toxicity, the lag phase was perceptible stating that both phenol and cyanide are inhibitory substrates. The absence of lag phase or existence of short initial lag phase at high substrate concentrations indicated that the microorganism can easily adapt to the aseptic environment. This can facilitate handling of enormous volumes of real industrial wastewater in practical applications at lower diametric vessels and capital input. It has been also mentioned that during the batch culture of microorganisms in the presence of substrate inhibition under inflated initial substrate concentrations, the exponential phase is usually short comparatively (Edward 1970). Literature also suggests that phenol-cyanide acclimatization of the microbial culture in advance has no lag phase existence for whatever may be the initial substrate concentrations [52]. The degradation of phenol and cyanide by the mixed strain of *Alcaligenes faecalis* JF339228 and *Klebsiella oxytoca* KF303807 with time is represented in Fig. 3c. A maximum degradation of 90.28% and 93.85% were observed in 40 h and 48 h for phenol and cyanide respectively.

3.2.2 Probable mechanism of cell growth and degradation

Biodegradation is a natural approach receiving gradual attention capable of persisting heavy shocks and loads during operation by activation of the biomass through aeration. The microorganism utilizes the organic waste as the food and energy source for essential metabolism and development as well as conversion into non virulent by-products. The following mechanism is responsible for degradation of the organic waste by the microbial community [64, 65]:

$$\text{Microorganism} + R + O_2 \rightarrow R^{\circ} + H_2O \quad (11)$$

$$\text{Microorganism} + R^{\circ} \rightarrow P + \text{BP} + \text{MG} \quad (12)$$

$$R^{\circ} + \text{Microorganism} \rightarrow R^{+} + \text{BP} + \text{MG} \quad (13)$$

$$R^{+} + H_2O \rightarrow P + H^{+} \quad (14)$$

R = pollutant; R° = oxidized radical due to electron release; R^{+} = intermediate product; P = degraded product like carbon dioxide; BP= some other secondary by-products; MG= more number of microbial cells.

The degradation kinetics has been considered in three consecutive stages: (1) phenol and cyanide transportation from bulk liquid phase to the surface of the microbial cell membrane; (2) transfer through cell membrane and entering into the cytoplasm layer adjacent to the cell membrane; (3) transport of phenol and cyanide to the enzymatic reaction site for utilization as nutrient source. Figure 4 represents the possible phenomena occurring within the bacterial structure. The total phenomena can be explained through mass transport equation as follows:

$$\text{Stage 1} : N_{A1} = k_{L1\,a1}\,(C^{*} - C_1) \quad (15)$$

$$\text{Stage 2} : N_{A2} = k_{L2\,a2}\,(C_1 - C_2) \quad (16)$$

$$\text{Stage 3} : N_{A2} = k_{L3\,a3}\,(C_2 - C_3) \quad (17)$$

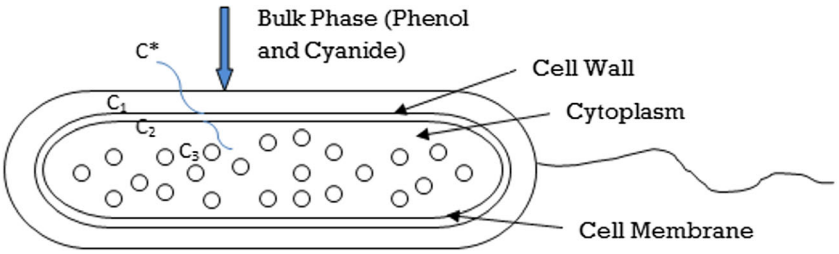

Fig. 4 Bacterial cellular structure showcasing the possible mass transport mechanism for intake of toxicants

where N_{A1}, N_{A2} and N_{A3} denote the mass fluxes; k_{L1}, k_{L2} and k_{L3} designate the mass transfer coefficient; and a_1, a_2 and a_3 signify the interfacial cellular area for stages 1, 2 and 3 respectively. C^* stands for bulk phase concentration, C_1 and C_2 are interfacial concentration and C_3 specifies the concentration at the cytoplasm side.

Initially at time t=0, C_1=0, C_2=C_3=0, with time C_1, C_2, C_3 increases. Ultimately, at steady state, the amount of toxicants reaching to the reaction site is converted to consumable simpler products like sugar and amino acids for cellular activities. In this study, the toxicants might have been absorbed by the cellular membrane to be transported from bulk side to reaction side by adsorption mechanism.

$$\begin{gathered}\text{At steady state}, N_{A1} = N_{A2} = N_{A3},\\ \text{or } k_{L1\,a1}\,(C^*{-}C_1) = k_{L2\,a2}\,(C_1{-}C_2) = k_{L3\,a3}\,(C_2{-}C_3)\\ \text{or}, N_A = k_L\,a\,(C_1{-}C_3)\end{gathered} \tag{18}$$

The above equation takes the form of linear equation y = mx and a similar trend is obtained in Fig. 3c where the mass flux N_A is typically high during the initial stage and reaches steady state finally.

3.3 Growth kinetic studies

The bacterial growth kinetics in phenol-cyanide substrate system was carried out to investigate the suitability of the deterministic kinetic growth models for the substrates. Results suggested that both the specific growth and substrate degradation rate is affected by substrate inhibition. Different growth kinetic models were selected for evaluation of the parameters as reported in Tables 2 and 3. This suggests that maximum specific growth rate values and inhibition coefficients were found reasonable with the literature [32, 36]. The half saturation coefficient ($K_{sphenol}$= 13.09 mg L^{-1}; $K_{scyanide}$= 21.759 mg L^{-1}) which is usually influential in the lower substrate region was found to be higher for both phenol and cyanide in comparison to phenol-*P. putida* systems (K_s=5.94 mg L^{-1}). However, the substrate inhibition coefficient ($K_{iphenol}$ =48.36 mg L^{-1}; $K_{icyanide}$= 59.43 mg L^{-1}) values were found to be in the medium range as reported for pure strains [52]. The maximum specific growth rates ($\mu_{max,phenol}$= 0.096 h^{-1}; $\mu_{max,cyanide}$=0.126 h^{-1}) were found to be higher than phenol-*Sulfolobus solfataricus* systems (0.047 h^{-1}). This is mainly due to the prior acclimatization of the co-cultured strains to phenol-cyanide environment which helps in improving it. A comparative representation obtained in the case of different kinetic models is expressed in Fig. 5a and b. The kinetic parameters obtained from the different models and SSEs between the predicted and experimental data were implemented to predict the applicability of the best fitted model. As outlined by Viggiani et al. [40], the substrate inhibition starts after 200 mg L^{-1} phenol. Similar results were also portrayed by Singh and Balomaumdar (2016b) with substrate inhibition resuming after 250 mg L^{-1} for phenol (μ_{max} = 0.0958 h^{-1}) and 25 mg L^{-1} for cyanide (μ_{max} = 0.1590 h^{-1}) using *Pseudomonas putida MTCC 1194*. The maximum specific growth rates in this case were slightly higher compared to the results obtained by the same group when performed with mixed strains like *P. putida MTCC 1194* and *S. odorifera MTCC 5700* where μ_{max} = 0.0663 h^{-1} for 250 mg L^{-1} phenol and 0.143 h^{-1} for 25 mg L^{-1} cyanide was observed [36]. Singh et al. [31] utilized *Pseudomonas putida* and *Pseudomonas stutzeri* strains by immobilization onto carbon matrix and could handle up to 1800 mg L^{-1} phenol and 340 mg L^{-1} cyanide simultaneously. These strains were not only successful in reducing the overall biological oxygen demand and chemical oxygen demand of the coke oven effluent but could deflate the alkalinity of the wastewater to neutral range. The excellent ability of *A. faecalis* JF339228 to handle 200 mg L^{-1} phenol and 20 mg L^{-1} cyanide in an immobilized binary substrate system has been reported by Pathak et al. [60].

A. faecalis JF339228 for phenol degradation in combination with a typically cyanide degrader like *K. oxytoca* KF303807 proved to be effective in administering high levels of toxicity [43]. All the models including Haldane, Edward and Aiba were found to be suitable for phenol and cyanide substrate growth kinetics. However, based on the lower SSE and correlation coefficient (R^2) values, Haldane model for phenol (0.0021; R^2= 0.9951) and Edward model for cyanide (0.0011; R^2 = 0.9986) suited best. Though all the SSE values were nearly close, in the case of cyanide, the value was improvised in Edward inhibitory model compared to Haldane. After review of the results obtained from different kinetic models, it is to be noted that there is a quantitative difference between the parameters (μ_{max}, K_s) but not from the qualitative

Table 2 Model growth kinetic parameters during biodegradation of phenol by mixed bacterial culture

Phenol						
Model	Model parameters μ_{max} (h^{-1})	K_s (mg L^{-1})	K_i (mg L^{-1})	S_m	SSE	R^2
Monod	0.1022	0.5067	–	–	0.0141	0.9896
Haldane	0.0916	13.0987	48.3604	25.168	0.0021	0.9951
Edward	0.098	19.139	68.276	36.148	0.0161	0.9849
Aiba	0.089	24.6734	76.4345	43.4269	0.0142	0.9940

aspects for inhibitory and non-inhibitory models. Both the components depicted high values of substrate inhibition constant K_i which means that the bacterial strains selected for the study was eligible for handling elevated toxic concentrations. Though Aiba model was less fitted compared to other two inhibition models, the K_i values calculated for phenol and cyanide were highest. Also in drawing a line of comparison between phenol and cyanide, the higher K_i values reflected more inhibitory effect of cyanide compared to phenol. S_m was found to be quite high in comparison to initial concentration of wastewater confirming the fact of suitability of the selected bacteria. Monod kinetics was not found suitable for both the toxicants since a higher working concentration range was selected which outlines the main limitation of the said model. Therefore, it becomes very crucial to select appropriate model and kinetic parameters for determining the fate of the toxicant transport. To interpret the interactions of the substrate inhibition in a binary substrate system, a nonlinear regression technique comprising of SKIP model was executed. In a binary component system containing phenol and cyanide, the specific growth rate for the bacterial consortium was expressed as [66, 67]:

$$\mu = \frac{0.0916S_1}{13.098 + S_1 + \frac{{S_1}^2}{48.3604} + 0.345S_2} + \frac{0.118S_2}{14.586 + S_2 + \frac{{S_2}^2}{66.9486} + 21.19S_1} \quad (19)$$

The interaction parameters as obtained from the model analysis indicated that the inhibitory effect of phenol was greater than cyanide in the case of cyanide degradation.

3.4 Fluorescence spectrophotometer analysis

The risk assessment of different virulent compounds becomes necessary to analyse the potential threat on human and aquatic systems. Also it is important to assess the treated effluent before final disposal as more secondary toxic intermediates might be produced after treatment. For instance, catechol is produced as a secondary intermediate during phenol degradation which is considered more toxic than phenol [29]. DNA is the commonly used target comprising of a double helical structure for studying the mode of interaction with the toxic molecules. There can be two types of binding: covalent binding which is irreversible causing complete DNA inhibition and cell death, and non-covalent binding as observed in this case is commonly applied for the study of DNA damage by toxicants. Both intercalation and groove binding were observed in this study. In the case of intercalation, unwinding of the helical DNA strands occur where Ethidium cation acts as the intercalator and the complex is stabilized by π-π interactions. This is less sensitive compared to groove binding where the small molecules settle in the grooves of the DNA by hydrogen bonding and Van der Waals forces.

Fluorescence spectroscopy is an efficient methodical tool for interpretation of DNA interaction with small ligand molecules and is extensively applied for aromatic, aliphatic functional groups or conjugated double-bond alicyclic carbonyl structures. DNA is interpolated by the fluorophore (EtBr) at the first binding point where solvable compounds are intercalated to the nucleic acid base pairs through groove binding producing enormous fluorescence. The second binding

Table 3 Model growth kinetic parameters during biodegradation of cyanide by mixed bacterial culture

Cyanide						
Model	Model parameters μ_{max} (h^{-1})	K_s (mg L^{-1})	K_i (mg L^{-1})	S_m	SSE	R^2
Monod	0.124	0.0701	–	–	0.0139	0.9945
Haldane	0.118	14.5867	66.9486	31.2499	0.014	0.9938
Edward	0.107	21.759	59.431	35.9605	0.0011	0.9986
Aiba	0.118	18.546	62.5464	34.0585	0.0121	0.9979

position demonstrates electrostatic interactions between cationic surfaces of EtBr with anionic phosphate groups on DNA [68]. The mutilation caused to DNA is revealed by the increase in fluorescence intensity until saturation or quenching phenomena (deflation in intensity) due to the addition of a secondary molecule. The inflation in intensity depends on the complex formation and number of non-covalent interreaction nodes [69]. On reaching the saturation, the increase in the intensity stops. Figure 6a showcases the emission spectra of the untreated and microbially treated samples by molecular probe EtBr-hs DNA. The increase in the intensity is due to the competitive intercalation effect of the secondary molecules that replaces the fluorophore EtBr. Results perceived from Fig. 5a explained that the increase in the wastewater concentration from 100:10 to 1500:150 mg L^{-1} caused

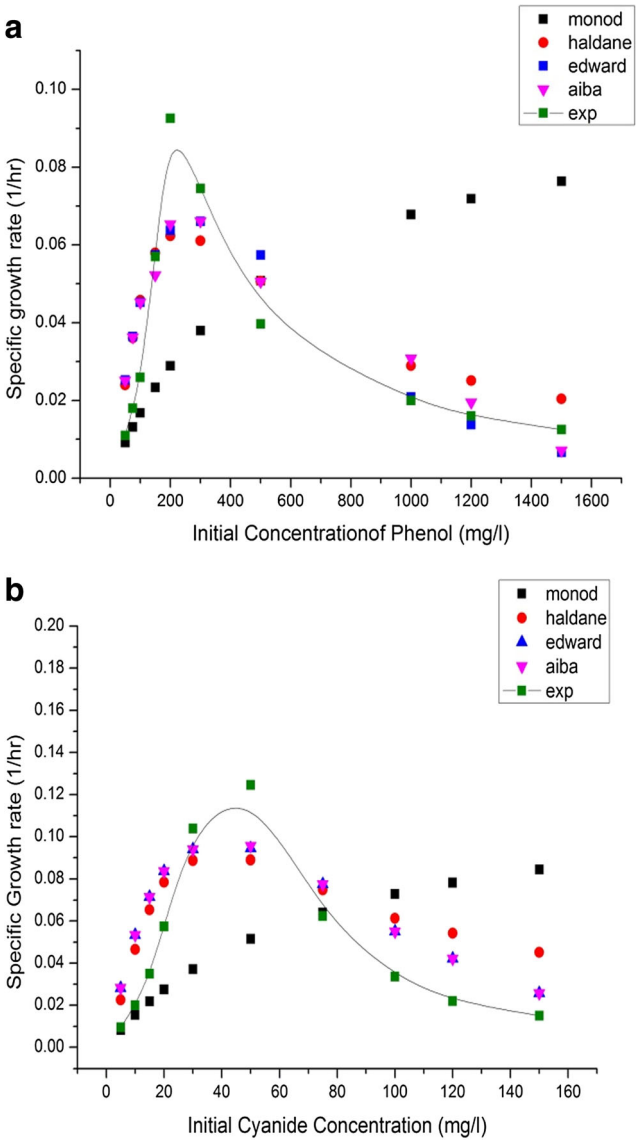

Fig. 5 A comparative study of experimental specific growth rate with different kinetic models for various **a** initial phenol concentrations and **b** initial cyanide concentrations

enhanced fluorescence by intercalation. However, the intensity of the treated sample was quite in accordance with the control (EB dye + hs-DNA) having no toxicants. The specimen containing free mixed consortium of bacteria had a fluorescence intensity increase due to some complex formation between the compounds present in the nutrient media with the DNA.

UV-visible absorption spectroscopy was employed to examine the exact mode of binding (groove or external) between the organic complex molecules and DNA. This provided better understanding of the toxicity and damaging effect of the pollutant molecules on DNA in combination with fluorescence spectroscopic analysis. The modifications in the absorption intensity and shifting of the bands in the visible spectrum as a result of interaction of the hs-DNA with complex molecules are distinguishable from a broad spectrum around 260 nm. This region constitutes the attachments of the chromophoric groups in the DNA base pairs comprising of purine and pyrimidine structures [68, 69]. Figure 6b demonstrates the absorption spectrum of the simulated wastewater with increasing concentration and treated sample in comparison to the control. Hyperchromism with slight red shift was observed in the case of the toxic wastewater with inflating concentration. This is a consequential effect of the denaturation of double-base DNA structure into single strands with conformational structural changes due to extreme toxicity [70]. The slight bathochromic or red shift outlines the electrostatic interactions which cause partial unfolding of the DNA stands with corresponding variations in the stacking pattern of the double helical structure [69, 71]. The similar above effect as perceived in the case of free cells was due to the strong intercalation and groove binding of the molecules with the hs-DNA produced by the mixed bacterial consortium in nutrient medium. In the case of the treated wastewater, hypochromism in combination with red shift signified moderate favourable electrostatic intercalation with maintenance of the DNA duplex structure [72].

3.5 Phytotoxicity studies and germination assay

The seed imbibition and inception of radical that further transforms into root constitutes germination process in plant species [73]. The germination process is perturbed due to complicated biochemical phenomena associated with stress-induced mutations [74]. The first emanation of the germination under different treatment is usually observed after 24 h in the seeds. In this research, the phytotoxicity studies were performed for three different concentrations of wastewater containing phenol:cyanide as 100:10 ppm, 500:50 ppm and 1500:50 ppm respectively. The treated wastewater sample after biodegradation was also considered for the study. Figure 7a and b illustrate the germination assay of the *V. radiata* under increasing concentration and bacterial treated

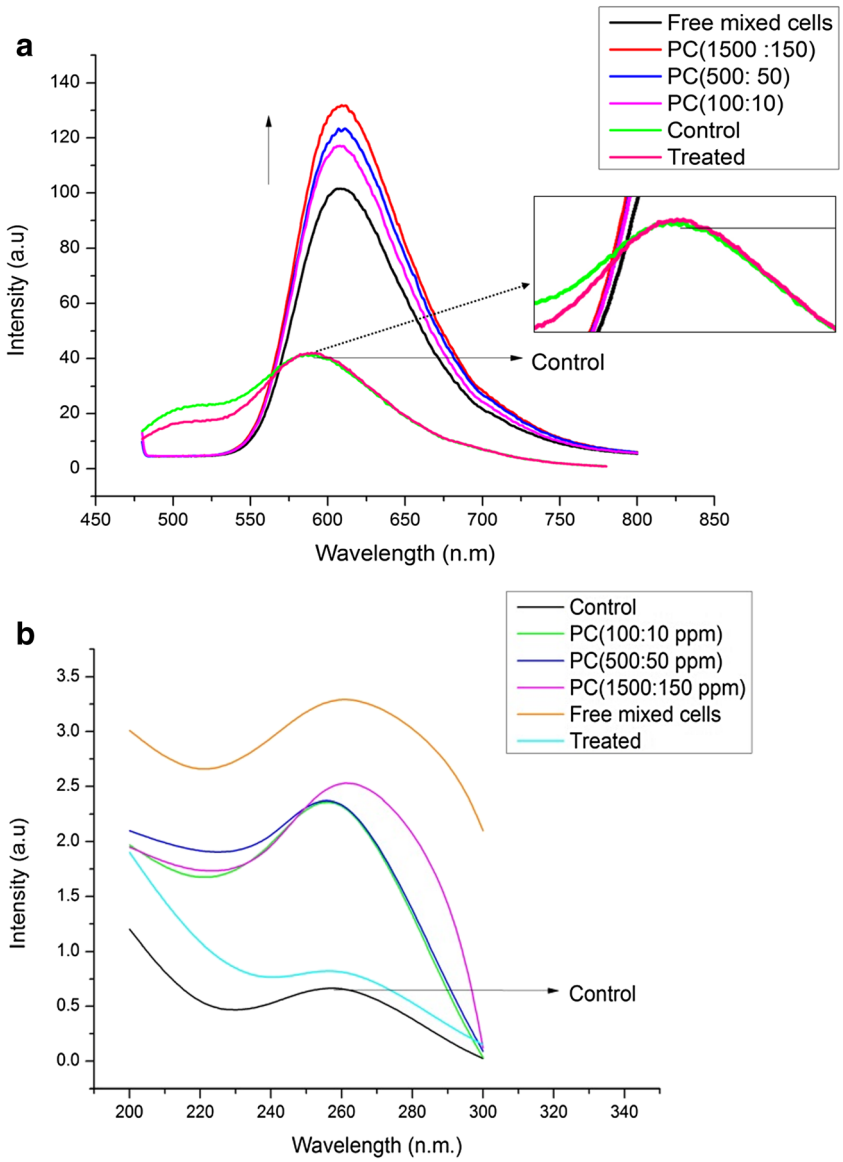

Fig. 6 **a** Fluorescence emission spectra of Herring sperm DNA-Ethidium Bromide dye complex in untreated and microbial treated phenol-cyanide system. **b** UV-visible absorption spectra of herring sperm DNA in untreated and microbial treated phenol-cyanide system

wastewater in comparison to control system. The untreated wastewater samples having phenol:cyanide concentrations 500:50 ppm and 1500:50 ppm showed higher phytotoxic impact in comparison to 100:10 ppm. The results suggested that the inhibitory action of phenol and cyanide on root and shoot system was around 90–99% indicating 3rd level of toxicity. The root and shoot inhibition observed in the case of 100:10 ppm of wastewater was 70–80% depicting same level of toxicity. However, the biologically treated specimen demonstrated inhibition due to germination below 50% which still implies a 2nd level of toxicity. Root and shoot toxicity of *V. radiata* seeds germinated in untreated and bacterial treated effluents were assessed and compared with reference control as represented in Fig. 8. With further exposure at increasing concentrations, a high percentage of inhibition in lengths of root and shoot length was observed. The germination in the case of untreated effluent significantly reduced due to vitiated metabolic activities within the seeds [75]. The percentage root and shoot toxicity were much lower in treated and control plates as compared to the untreated wastewater. Several researches are being carried out on plant growth model and genotoxicity of steel plant wastewater [76, 77]. Smol et al. [78] performed phytotoxicity analysis of coke oven wastewater using raw effluent and treated specimen from biological, sand bed filtration and reverse osmosis (RO) membrane units. The test was conducted on a *Vicia faba* which showed strong toxic effects in the case of raw effluent compared to sand bed and RO-treated samples. The membrane treated effluent showed 85% reduction in chemical oxygen demand (COD) and 95% in total organic carbon (TOC). In addition, they concluded that the practical sample collected from real industrial units will always have profound toxic impact even after

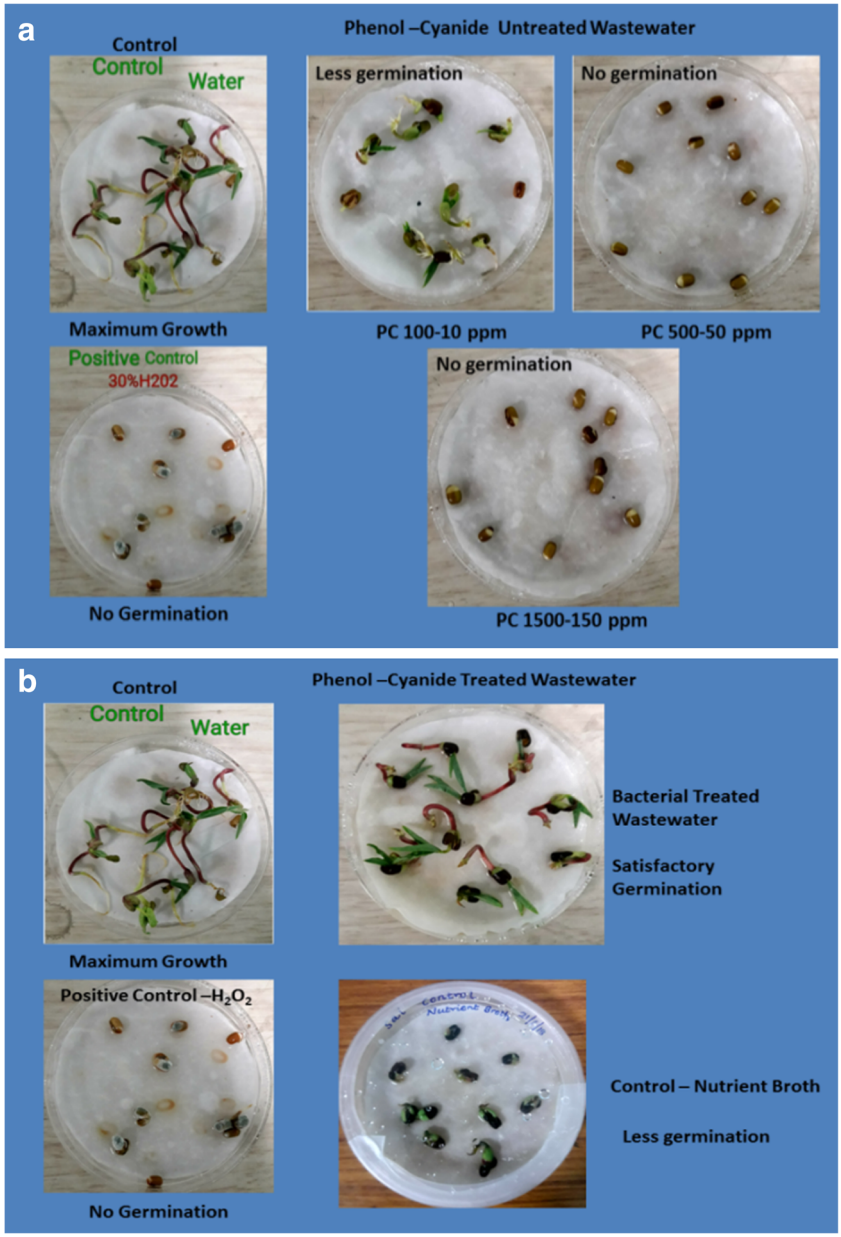

Fig. 7 **a** Phytotoxicty studies of untreated wastewater containing phenol and cyanide. **b** Phytotoxicty studies of treated wastewater

treatment. That means even after drastic reduction of COD and TOC following advanced treatment techniques, the wastewater may contain hazardous compounds not preferable for the life of flora and fauna or human systems.

4 Conclusion

The present study depicted propitious results for bioremediation of phenol and cyanide using the mixed cultures. The bacterial growth and degradation kinetics validated using the experimental data displayed inherent remediation up to 450 mg L^{-1} of phenol (90.28% in 40 h) and 45 mg L^{-1} of cyanide (93.85% in 48 h) with favourable fit for the applied substrate inhibition models. The results obtained from toxicological study with the bacterial remediated effluent indicated preferential adoption of the biodegradation strategy using mixed culture for eco benign disposal. Thus, the overall observations stipulated the efficacy of the isolated bacterial strains *A. faecalis* JF339228 and *K. oxytoca* KF303807 for bioattenuation of severely pernicious phenol and cyanide to explore its application on a scaled-up designed culture operation in future. Selection of the proper target-specific microorganism and optimization of the artificial degradation environment is essential for treating these high concentration complex wastewaters in industrial systems Designing of suitable bioreactors setup for bioaugmentation of biological units can be achieved to overcome the conventional activated sludge

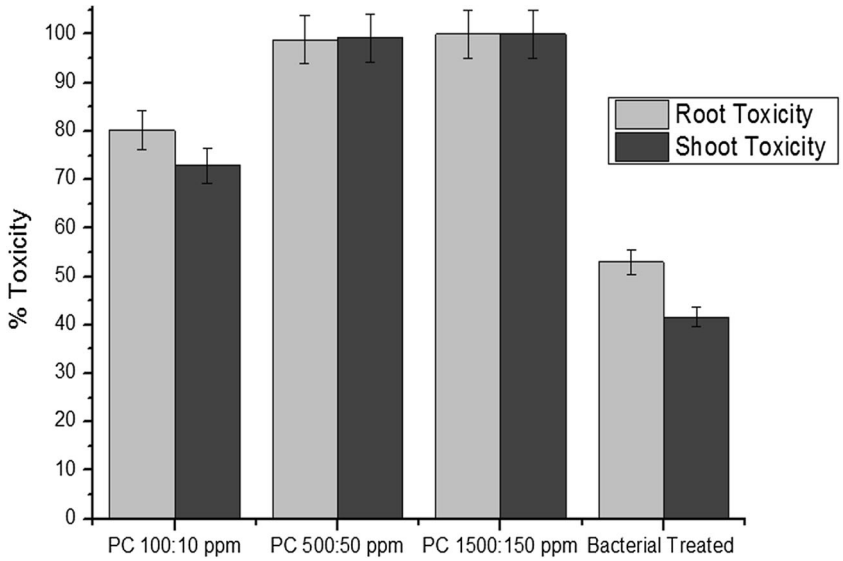

Fig. 8 Root and shoot toxicity of *V. radiata* seeds germinated in untreated and bacterial treated effluents

system. However, microbial activity still remains a "Black box" where addressal of technical issues is a challenge in practical systems and a single bioreactor is insufficient for treatment of these toxic effluents. Thus, it is important to find a cost-effective sustainable solution for suitable discharge into the ecosystem or reuse within the plant units as an alternative to clean water.

Acknowledgements The authors are grateful to the Ministry of Human resource Development (MHRD), Government of India and Department of Science and Technology India for extending instrumental facility with reference to DST-FIST project number SR/FST/ETI-405/2015 (C)/NIT Durgapur.

Declarations

Conflict of interest The authors declare no competing interests.

References

1. Aksu Z, Yener J (2001) A comparative adsorption/biosorption study of mono chlorinated phenols onto various sorbents. Waste Manag 21:695–702
2. Aleksieva, Z., Ivanova, D., Godievargova, T., Atanasov, B. (2002). Degradation of some phenol derivatives by Trichosporon cutaneum R57. Process Biochem, 37, 1215–1219.
3. Busca G, Berardinelli S, Resini C, Arrighi L (2008) Technologies for the removal of phenol from fluid streams: a short review of recent developments. J Hazard Mater 160:265–288
4. Calace N, Nardi E, Petronio BM, Pietroletti M (2002) Adsorption of phenols by paper mill sludges. Environ Pollut 118:315–319
5. Desai JD, Ramakrishna C (1998) Microbial degradation of cyanides and its commercial application. J Sci Ind Res 57:441–453
6. Patil YB, Paknikar KM (2000) Development of a process for bio detoxification of metal cyanides from wastewater. Process Biochem 35:1139–1151
7. Rao JR, Viraraghavan T (2002) Biosorption of phenol from an aqueous solution by Aspergillus niger biomass. Bioresour Technol 85:165–171
8. Kim MY, Park D, Jeon CO, Lee SD, Park MJ (2008) Effect of HRT on biological pre denitrification process for the simultaneous removal of toxic pollutants form cokes wastewater. Bioresour Technol 99:8824–8832
9. Qiang LH, Jun HH, An DM, Wei W (2011) Removal of phenols, thiocyanate and ammonium from coal gasification wastewater using moving bed biofilm reactor. Bioresour Technol 102(7): 4667–4673
10. Vedula RK, Dalal S, Majumder CB (2013) Bioremoval of cyanide and phenol from industrial wastewater: an update. Biorem J 17(4): 278–293
11. Dash RR, Balomajumder C, Kumar A (2009) Removal of cyanide from water and wastewater using granular activated carbon. Chem Eng J 146:408–413
12. Rittmann BE, McCarty PL (2001) Environmental biotechnology, in Series Water Resources and Environmental Engineering. Mc Graw Hill 5:261–306
13. ATSDR (2006) Agency for toxic substances and Disease Registry. Public Health Statement, Cyanide
14. ATSDR (2008) Agency for toxic substances and Disease Registry. Toxicological profile for phenol, US, Department of Health and Human Service
15. Caetano M, Valderrama C, Farran A, Cortina JL (2009) Phenol removal from aqueous solution by adsorption and ion exchange mechanisms onto polymeric resins. J Colloid Interface Sci 338: 402–409
16. Hsieh CT, Teng H (2000) Liquid-phase adsorption of phenol onto activated carbons prepared with different activation levels. J Colloid Interface Sci 230:171–175
17. Botz, M.M. (2001). Overview of cyanide treatment methods, in: Mining Environmental Management. Mining Journal Ltd. pp.28–30. London, UK.
18. Juttner K, Galla U, Schmieder H (2000) Electrochemical approaches to environmental problems in the process industry. Electrochim Acta 45:2575–2594
19. Kujawski W, Warszawski A, Ratajczak W, Porebski T, Capala W (2004) Removal of phenol from wastewater by different separation techniques. Desalination 163:287–296

20. Tomaszewska M, Mozia S, Morawski W (2004) Removal of organic matter by coagulation enhanced with adsorption on PAC. Desalination 162:79–87
21. Yang LP, Hu WY, Huang HM, Yan B (2010) Degradation of high concentration phenol by ozonation in combination with ultrasonic irradiation. Desal Water Treat 21:87–95
22. Felföldi T, Nagymáté Z, Székely AJ et al (2020) Biological treatment of coke plant effluents: from a microbiological perspective. Biologia Futura 71:359–337. https://doi.org/10.1007/s42977-020-00028-2
23. Bai J, Wen JP, Li HM, Jiang Y (2007) Kinetic modelling of growth and biodegradation of phenol and m-cresol using *Alcaligenes faecalis*. Process Biochem 42:510–517
24. Kumar A, Priyadarshinee R, Singha S, Sengupta B, Roy A, Dasgupta D, Mandal T (2019) Biodegradation of alkali lignin by Bacillus flexus RMWW II: analyzing performance for abatement of rice mill wastewater. Water Sci Technol 80:9
25. Akcil A (2003) Destruction of cyanide in gold mill effluents: biological versus chemical treatments. Biotechnol Adv 21:501–511
26. Aisami A, Gusmanizar N, Rusnam M, Syed MA, Shamaan NA, Shukor MY (2020) Remodelling the growth inhibition kinetics of Pseudomonas sp. strain DrY Kertih on Acrylamide. BSTR 8(2):16–20
27. Akcil A, Karahan AG, Ciftci H, Sagdıc O (2003) Biological treatment of cyanide by natural isolated bacteria (Pseudomonas sp.). Miner Eng 16:643–649
28. Allsop PJ, Chisti Y, Young MM, Sullivan GR (1993) Dynamics of phenol degradation by Pseudomonas putida. Biotechnol Bioeng 41:–572
29. Kumar A, Kumar S, Kumar S (2005) Biodegradation kinetics of phenol and catechol using *Pseudomonas putida* MTCC. Biochem Eng J 22:151–159
30. Zhu S, Wu H, Zhou L, Wei C (2017) The resilience of microbial community involved in coking wastewater treatment system. Next Gener Seq Appl 4:1
31. Singh U, Arora NK, Sachan P (2018) Simultaneous biodegradation of phenol and cyanide present in coke-oven effluent using immobilized *Pseudomonas putida and Pseudomonas stutzeri*. Braz J Microbiol 49:38–44. https://doi.org/10.1016/j.bjm.2016.12.013
32. Singh N, Balomajumder C (2016b) Biodegradation of phenol and cyanide by Pseudomonas putida MTCC 1194: an experimental and modeling study. Desalin Water Treat:1–10. https://doi.org/10.1080/19443994.2016.1179676
33. Aisami A, Usman MM (2020) Utilization of comprehensive mathematical modelling to evaluate the growth kinetics of Pseudomonas putida LY1 on Phenol. JOBIMB 8(1):37–41
34. Aisami A, Yasid NA, Johari WLW, Shukor MY (2017) Estimation of the Q10 value; the temperature coefficient for the growth of Pseudomonas sp. AQ5-04 on Phenol. BSTR 5(1):24–26
35. Aisami A, Yasid NA, Johari WLW, Ahmad SA, Shukor MY (2019) Growth rate abolishment on phenol as a substrate by Pseudomonas sp. AQ5-04 best modelled using the Luong substrate inhibition kinetics. Desalin Water Treat 152:214–220
36. Singh N, Balomajumder C (2016a) Batch growth kinetic studies for elimination of phenol and cyanide using mixed microbial culture. Journal of Water Process Engineering 11:130–137
37. Mandal S, Bhunia B, Kumar A, Dasgupta D, Mandal T, Datta S, Bhattacharya P (2013) A statistical approach for optimization of media components for phenol degradation by Alcaligenes faecalis using Plackett–Burman and response surface methodology. Desalin Water Treat 51(31-33):6058–6069
38. Kumar A, Bhunia B, Dasgupta D, Mandal T, Datta S, Bhattacharya P (2013) Optimization of culture condition for growth and phenol degradation by *Alcaligenes faecalis* JF339228 using Taguchi methodology. Desalin Water Treat 51:3153–3161
39. Ziembińska-Buczyńska A, Ciesielski S, Żabczyński S, Cema G (2019) Bacterial community structure in rotating biological contactor treating coke wastewater in relation to medium composition. Environ Sci Pollut Res 26:19171–19179
40. Viggiani, A., Olivieri, G., Siani, L., Di Donato, A., Marzocchella, A., Salatino, P., Barbieri, P., Galli, E. (2006). An airlift biofilm reactor for the biodegradation of phenol by *Pseudomonas stutzeri* OX1. J Biotechnol, 123, 464–477.
41. Tepe O, Dursun AY (2008) Combined effects of external mass transfer and biodegradation rates on removal of phenol by immobilized *Ralstonia eutropha* in a packed bed reactor. J Hazard Mater 151:9–16
42. Prieto M, Hidalgo AJ, Serra L, Llama MJ (2002) Degradation of phenol by Rhodococcus erythropolis UPV-1 immobilized on Biolite in a packed-bed reactor. J Biotechnol 97:1–11
43. Kao CM, Liu JK, Lou HR, Lin CS, Chen SC (2003) Biotransformation of cyanide to methane and ammonia by Klebsiella oxytoca. Chemosphere 50:1055–1061
44. Dwivedi N, Balomajumder C, Mondal P (2016) Comparative evaluation of cyanide removal by adsorption, biodegradation, and simultaneous adsorption and biodegradation (SAB) process using *Bacillus cereus* and almond shell. J Environ Biol 37:551–556
45. Meyers PR, Gohool P, Rawling DE, Wood DR (1991) An efficient cyanide degrading Bacillus pumilus strain. J Gen Microbiol 137:1397–1400
46. Kunz, D.A., Nagappan, O., Silva-Avalos, J., Delong, G.T., (1992) Utilization of cyanide as a nitrogenous substrate by *Pseudomonas fluorescens NCIMB 11764*: evidence for multiple pathways of metabolic conversion. Appl. Environ. Microbiol., 58, 2022–2029.
47. APHA (2005) Standard methods for the examination of water andwastewaters, 21st edn. APHA, AWWA, WPCF, Washington, DC
48. Ojaghi A, Tonkaboni SZS, Shariati P, Ardejani FD (2018) Novel cyanide electro-biodegradation using *Bacillus pumilus ATCC 7061* in aqueous solution. J Environ Health Sci Eng 16(2):99–108. https://doi.org/10.1007/s40201-018-0289-3
49. Muloiwaa M, Nyende-Byakikab S, Dinkab M (2020) Comparison of unstructured kinetic bacterial growth models. South African Journal of Chemical Engineering 33:141–150
50. Monod J (1949) The growth of bacterial cultures. Annu Rev Microbiol 3:371–394
51. Wang SJ, Loh KC (1999) Modeling the role of metabolic intermediates in kinetics of phenol biodegradation. Enzym Microb Technol 25:177–184
52. Christen P, Vega A, Casalot L, Simon G, Auria R (2012) Kinetics of aerobic phenol biodegradation by the acidophilic and hyperthermophilic archaeon Sulfolobus solfataricus 98/2. Biochem Eng J 62:56–61
53. Edwards VH (1970) The influence of high substrate concentrations on microbial kinetics. Biotechnol Bioeng 12:679–712
54. Mulchandani A, Luong JHT (1989) Microbial inhibition kinetics revisited. Enzym Microb Technol 11:66–73
55. Aiba S, Shoda M, Nagatani M (1968) Kinetics of product inhibition in alcohol fermentation. Biotechnol Bioeng 10:845–856
56. Kumar A, Priyadarshinee R, Singha S, Dasgupta D, Mandal T (2016) Rice husk ash based silica supported iron catalyst coupled with Fenton-like process for the abatement of rice mill wastewater. Clean Techn Environ Policy 18:2565–2577
57. Mishra V, Balomajumder C, Agarwal VK (2013) Design and optimization of simultaneous biosorption and bioaccumulation (SBB) system: a potential method for removal of Zn(II) ion from liquid phase. Desalin Water Treat 51:3179–3188
58. Nath J, Ray L (2015) Biosorption of Malachite green from aqueous solution by dry cells of Bacillus cereus M116 (MTCC 5521). J Environ Chem Eng 3:386–394

59. Nikiyan, H., Vasilchenko, A., Deryabin, D. (2010). AFM investigations of various disturbing factors on bacterial cells. in: A., Mén¬dez-Vilas, J. Díaz, (Eds.), Microscopy: Science, Technology, Applications and Education, pp. 523–529. Formatex Research Center, Spain.
60. Pathak U, Roy A, Mandal DD, Das P, Kumar T, Mandal T (2018) Bioattenuation of phenol and cyanide involving immobilized spent tea activated carbon with Alcaligenes faecalis JF339228 -Critical assessment of the degraded intermediates. Asia Pac J Chem Eng 14(1):e2278. https://doi.org/10.1002/apj.2278
61. Yan J, Jianping W, Jing B, Daoquan W, Zongding H (2006) Phenol biodegradation by the yeast Candida tropicalis in the presence of m-cresol. Biochem Eng J 29:227–234
62. Harayama S, Rekik M (1989) Bacterial aromatic ring-cleavage enzymes are classified into two different gene families. J Biol Chem 264:15328–15333
63. Toyama T et al (2009) Enrichment of bacteria possessing catechol dioxygenase genes in the rhizosphere of Spirodela polyrrhiza: a mechanism of accelerated biodegradation of phenol. Water Res 43(15):3765–3776. https://doi.org/10.1016/j.watres.2009.05.045
64. Mandal T, Dasgupta D, Datta S (2010) A biotechnological thrive on COD and chromium removal from leather industrial wastewater by the isolated microorganisms. Desalin Water Treat 13:382–392. https://doi.org/10.5004/dwt.2010.996
65. Sarkar KK, Majee S, Pathak U, Polepali S, Halder G, Mandal DD, Mandal T (2019) Development of an integrated treatment strategy for removal of ondansetron using simultaneous adsorption, oxidation and bioremediation technique. Journal of Environmental Chemical Engineering 7:103020
66. Reardon KF, Mosteller DC, Rogers JD (2000) Biodegradation kinetics of benzene, toluene and phenol and mixed substrates for Pseudomonas putida F1. Biotechnol Bioeng 69:385–400
67. Yoon H, Klinzing G, Blanch HW (1977) Competition for mixed substrates by microbial populations. Biotechnol Bioeng 19:1193–1210
68. Sirajuddin M, Ali S, Badshah A (2013) Drug–DNA interactions and their study by UV–visible, fluorescence spectroscopies and cyclic voltametry. J Photochem Photobiol B Biol 124:1–19
69. Benesi HA, Hildebrand JH (1949) Spectrophotometric investigation of the interaction of iodine with aromatic hydrocarbons. J Am Chem Soc 71(8):2703–2707
70. Arjmand F, Jamsheera A (2011) DNA binding studies of new valine derived chiral complexes of tin (iv) and zirconium (iv). Spectrochim Acta A 78:45–51
71. Sirajuddin M, Ali S, Shah NA, Khan MR, Tahir MN (2012) Synthesis, characterization, biological screenings and interaction with calf thymus DNA of a novel azomethine 3-((3,5-dimethylphenylimino) methyl)benzene-1,2-diol. Spectrochim Acta A 94:134–142
72. Kelly TM, Tossi AB, Mc Connel DJ, Streakas TC (1985) A study of the interactions of some polypyridylruthenium (II) complexes with DNA using fluorescence spectroscopy, topoisomerisation and thermal denaturation. Nucleic Acids Res 13:6017–6034
73. Nonogaki H, Bassel GW, Bewley JD (2010) Germination—still a mystery. Plant Sci 179:574–581
74. Wei H, Song S, Tian H, Liu T (2014) Effects of phenanthrene on seed germination and some physiological activities of wheat seedling. Comptes rendus biologies 337:95–100
75. Bhattacharya P, Mallick K, Ghosh S, Banerjee P, Mukhopadhyay A, Bandyopadhyay S (2014) Algal biomass as potential biosorbent for reduction of organic load in gray water and subsequent reuse: effect on seed germination and enzyme activity. Biorem J 18:56–70
76. Adamcová D, Vaverková MD, Břoušková E (2016) The toxicity of two types of sewage sludge from wastewater treatment plant for plants. Journal of Ecological Engineering 17(2):33–37
77. Sindera P, Felis E, Wiszniowski J (2011) Genotoxicity of coke wastewaters (Ocena genotoksyczności ścieków koksowniczych). Scientific Review–Engineering and. Environ Sci 53:217–225 (in Polish)
78. Smol M, Włóka D, Włodarczyk-Makuła M (2018) Influence of integrated membrane treatment on the phytotoxicity of wastewater from the coke industry. Water Air Soil Pollut 229:154